





Control of Mutual Coupling in Microstrip Antenna Design Based on Bio-inspired Algorithms

Israel Leal¹, Waslon Lopes², Marcelo Alencar¹, Wamberto Queiroz¹

¹Department of Electrical Engineering, Institute of Advanced Studies in Communications, Federal University of Campina Grande, Campina Grande, PB, Brazil, e-mails: israel.leal@ee.ufcg.edu.br; malencar@dee.ufcg.edu.br; wamberto@dee.ufcg.edu.br

²Department of Electrical Engineering, Center of Alternative and Renewable Energy, Federal University of Paraíba, João Pessoa, PB, Brazil, e-mail: waslon@ieee.org

Abstract— This paper presents a model that uses bio-inspired optimization algorithms to control of the mutual coupling (MC) in Multiple-Input Multiple-Output (MIMO) systems. The method promotes an increase in the channel throughput and a reduction in the distance among the array elements, searching values less than a half wavelength. A microstrip antenna design, at the frequency of 26 GHz, is used as a prototype for MIMO system testing and performance analysis. Genetic Algorithm (GA) is used to optimize, to determine the antenna physical parameters and to improve its performance. The mutual impedance concept is used to model the MC. The particle swarm optimization (PSO) algorithm is used to optimize the channel throughput and to reduce the distance between the elements. Simulation results show that it is possible to obtain a MIMO system performance improvement of 11.1% in channel throughput, the microstrip width is reduced by 14.5% and the distance among the elements can be reduced by 23.7%, considering the MC.

Index Terms— Bio-inspired algorithms, channel throughput, MIMO systems, mutual coupling.

I. INTRODUCTION

In recent years, the number of mobile data network users has grown at a steady pace worldwide, and this has largely increased the number of connections and equipments. According to the Group Speciale Mobile Association (GSMA), there were 5.3 billion mobile users around the world by the end of 2021. The Fourth Generation (4G) network has 58% of connections (excluding licensed cellular technology and Internet of things) and Fifth Generation (5G) network technology is already in use in 70 countries around the world [1].

The MIMO technique, which uses antenna arrays in transmission and reception, increases the transmission rate and is poised to achieve the radio channel transmission limits required in modern wireless networks [2]. The concept of MIMO systems brings new challenges for fifth generation (5G) networks, with the massive increase in the number of antennas and the corresponding research associated with its performance [3]–[5].

Some researchers use GA to optimize antennas, in microstrip design, by changing their physical dimensions and the format of the patches array [6], or by the minimization and evaluation of a single rectangular patch [7], [8]. In [9], the authors also use GA for linear optimization of an antenna array.

The PSO technique has been widely used in multiple antenna systems troubleshooting to find the best beamforming coefficients [4], to optimize the channel transmission rate without mutual coupling (MC) [5], [10], [11], in millimeter wave channel, to reduce the propagation loss [12]. In this work, PSO is proposed to optimize the microstrip antenna design considering the channel transmission rate and the MC between the antenna elements, reducing the distance between them.

An optimization methodology is proposed to design the system in this work. A change in the search algorithm for the sample space is performed to determine the MC influence between elements of the antenna, reducing the distance between them and maintaining the optimization of the transmission rate in the MIMO channel.

This work is organized as follows: the MIMO system channel gain matrix is presented in Section II and the MC effect is described in Section III. Section IV presents the fundamentals of the antenna design and some common antenna configurations. The work methodology using bio-inspired algorithms and the simulation setup are presented in Section V. Section VI presents the results of simulation and the conclusions of this paper are presented in Section VII.

II. THE CHANNEL GAIN MATRIX

Taking advantage of the spatial diversity through antenna arrays in MIMO systems, it assumes that the use of an antenna array increases the performance of the system by ensuring that the signal will reach the receiver with an appropriate Signal-to-Noise Ratio (SNR). MIMO systems exploit the multipath phenomenon to increase the transmission rate in environments that are highly influenced by reflection and diffraction propagation mechanisms. Depending on the number of antennas in the transmitter and receiver, the transmission rate may increase as a result of an increased complexity of the transmitted signal [13].

Considering a MIMO system characterized by a complex-valued matrix \mathbf{H} , the output signal is given by [2], [14], [15]

$$Y = \mathbf{H}\mathbf{x} + \mathbf{n}, \quad (1)$$

in which the input signal and the additive white Gaussian noise are represented by \mathbf{x} and \mathbf{n} , respectively [15]. The transmitter is assumed to be subject to an average power constraint of P across all transmit antennas. Since the noise power is normalized to unity, one commonly refers to the power constraint P as the SNR [14].

The perfect channel state information at the transmitter (CSIT) and at the receiver (CSIR) model is justified by the scenario where the channel state can be accurately tracked at the receiver and the statistical channel model at the transmitter is based on information about the channel gain probability distribution fed back from the receiver. Considering perfect CSIT and CSIR, the ergodic capacity of the MIMO channel is given by [14], [16]

$$C = E \left[\log_2 \left(\det \left(\mathbf{I}_{N_r} + \frac{P}{N_t} \mathbf{H}\mathbf{H}^H \right) \right) \right], \quad (2)$$

in which the identity matrix of order N_r is represented by \mathbf{I}_{N_r} , $E[\cdot]$ is expected value operator, $(\cdot)^H$ represents the Hermitian transposition of the channel gain matrix \mathbf{H} considering N_r and N_t the number of receive and transmit antennas, respectively. Finally, P is the transmitting power [14], [16].

This research uses the Kronecker channel model to compute the channel gain matrix \mathbf{H} [15], [17]–[19]. Correlation matrixes in reception and transmission are considered separable and they can be

calculated by

$$\mathbf{H} = \mathbf{R}_Y^{1/2} \mathbf{G}_H \mathbf{R}_X^{1/2}, \quad (3)$$

in which the spacial correlation in receiver and transmitter are represented by \mathbf{R}_Y and \mathbf{R}_X , respectively, and \mathbf{G}_H is a Gaussian matrix with elements characterized by identical and independently distributed (i.i.d) Gaussian random variables with zero mean and unit variance [15], [20].

In order to compute the channel gain matrix as a function of the transmitter and receiver impedances it is necessary to adapt Equation (3). This is possible using

$$\mathbf{H}_1 = \mathbf{Z}_r^{-1} \mathbf{H} \mathbf{Z}_t^{-1}, \quad (4)$$

in which \mathbf{H}_1 is the new gain matrix with the MC effect considered, \mathbf{Z}_r and \mathbf{Z}_t are the mutual impedances in the receiver and transmitter, respectively [21].

III. MUTUAL COUPLING

Antenna spacing, in the antenna array, is known to influence spatial correlation which limits the channel throughput increase [22]. This finite spacing is also responsible for the MC that affects signal transmission and reception due to antenna impedance mismatch. The effect of MC is especially pronounced in arrangements with elements spaced less than $\lambda/2$. Due to the considerable demand for compacting the size of mobile systems, the effect of MC cannot be overlooked [15].

The mutual impedance concept is used for evaluating the MC effect on antenna arrays. This paper describes the effects of MC on antenna arrays in reception and transmission, and uses the conventional mutual impedance method (CMIM) [23] and the corresponding receiving mutual impedance method (RMIM) [24] in the design of the transmission and reception antenna arrays.

Conventionally, it is defined the mutual impedance between two elements as shown in Fig. 1 [22], i.e, a transmission antenna connected to one source and a reception antenna is in a open circuit [25]. Due to the MC effect, there are two additional sources of excitation in the equivalent circuits. The MC

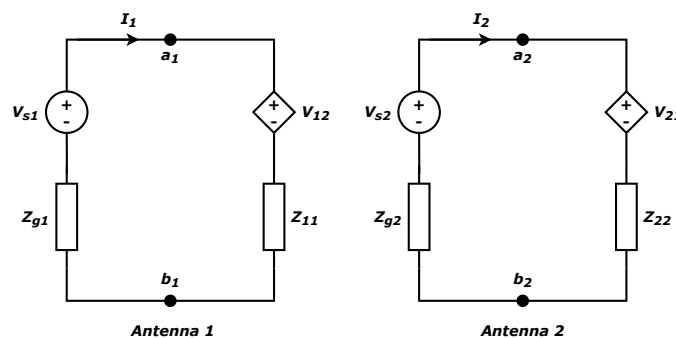


Fig. 1. Equivalent circuit of two receiving antennas considering MC. Adapted from [22].

effect is modeled using the controlled voltage sources V_{12} and V_{21} in the equivalent circuit. They can be obtained from the currents I_1 and I_2 in both antennas, such as [22]

$$V_{12} = \frac{I_2 Z_{12}^T}{Z_A} (Z_{in} + Z_g), \quad V_{21} = \frac{I_1 Z_{21}^T}{Z_A} (Z_{in} + Z_g), \quad (5)$$

in which Z_{in} and Z_g are the antennas input impedance and the source impedance. The coupled voltage of the Antenna 1 and Antenna 2 are represented by V_{12} and V_{21} , considering the terminal with open

circuit. The excitation current of the Antenna 1 and Antenna 2 are represented by I_1 and I_2 considering the terminal with short-circuit, respectively.

The mutual impedances can be described as [22], [24]

$$Z_{12} = \frac{V_{12}}{I_2} = \frac{V_{12}Z_A}{I_2(Z_{in} + Z_g)} \quad (6)$$

and

$$Z_{21} = \frac{V_{21}}{I_1} = \frac{V_{21}Z_A}{I_1(Z_{in} + Z_g)}, \quad (7)$$

in which Z_{12} and Z_{21} represent the mutual impedance excited in Antenna 2 and Antenna 1, respectively.

Expressions (8) and (9) describe the total voltage generated by the excitation sources and coupling,

$$V_{T1} = V_{s1} - V_{12} = I_1(Z_{g1} + Z_{11}) \quad (8)$$

and

$$V_{T2} = V_{s2} - V_{21} = I_2(Z_{g2} + Z_{22}), \quad (9)$$

respectively.

For N elements in a transmitter antenna array, the excitation voltages without considering MC, V_{s1} , V_{s2} , ..., V_{sN} are related to V_{T1} , V_{T2} , ..., V_{TN} , as follows [26]

$$\begin{bmatrix} V_{s1} \\ V_{s2} \\ \vdots \\ V_{sN} \end{bmatrix} = \begin{bmatrix} 1 & \frac{Z_{1,2}}{Z_{g2}+Z_{22}} & \cdots & \frac{Z_{1,N}}{Z_{gN}+Z_{NN}} \\ \frac{Z_{2,1}}{Z_{g1}+Z_{11}} & 1 & \cdots & \frac{Z_{2,N}}{Z_{gN}+Z_{NN}} \\ \vdots & \vdots & \ddots & \vdots \\ \frac{Z_{N,1}}{Z_{g1}+Z_{11}} & \frac{Z_{N,2}}{Z_{g2}+Z_{22}} & \cdots & 1 \end{bmatrix} \begin{bmatrix} V_{T1} \\ V_{T2} \\ \vdots \\ V_{TN} \end{bmatrix}. \quad (10)$$

The RMIM method, different from CMIM, considers an impedance Z_L terminated in the antenna elements and an external planar wave exciting these elements in receive mode [24], [26].

Fig. 2 shows the equivalent circuit of dipoles in the receive mode. It is possible to observe that the definition of mutual impedance at the reception implies that it depends on the direction of an idealized plane wave that is used as the excitation source. But for omni-directional antennas, for instance, in the dipole or monopole antenna, the mutual impedance at reception is independent of the azimuth angle of the plane wave [25]. From this scenario, the following results are obtained:

$$Z_r^{12} = \frac{-V_{12}}{I_2} \quad \text{and} \quad Z_r^{21} = \frac{-V_{21}}{I_1}, \quad (11)$$

in which Z_r^{12} and Z_r^{21} are the mutual impedances in the receive mode in Antenna 1 and Antenna 2. V_{12} and V_{21} are the voltages coupled of Antenna 1 and Antenna 2m. Finally, I_1 and I_2 are the currents received on Antenna 1 and Antenna 2, respectively [25].

The received voltages across the elements of Antenna 1 and Antenna 2 can be calculated by using (12) and (13). Considering U_1 and U_2 , the voltages of the isolated terminal in Antenna 1 and Antenna 2 without coupled voltages V_{12} and V_{21} , respectively, then [25]

$$V_1 = U_1 + V_{12} = U_1 - Z_r^{12}I_2 = U_1 + Z_r^{12} \frac{V_2}{Z_L} \quad (12)$$

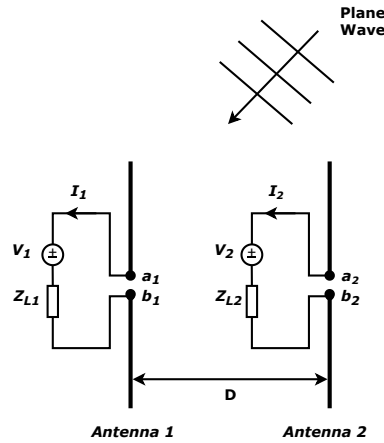


Fig. 2. Two dipoles antennas in reception mode. Adapted from [25].

and

$$V_2 = U_2 + V_{21} = U_2 - Z_r^{21} I_1 = U_2 + Z_r^{21} \frac{V_1}{Z_L}, \quad (13)$$

respectively.

Equation (14) expresses the relation between V_k and U_k , considering an antenna array with N elements in the receive mode. V_k and U_k are the voltage in the antenna terminal and the voltage produced by external source, respectively.

$$\begin{bmatrix} U_1 \\ U_2 \\ \vdots \\ U_N \end{bmatrix} = \begin{bmatrix} 1 & -\frac{Z_r^{12}}{Z_L} & \cdots & -\frac{Z_r^{1N}}{Z_L} \\ -\frac{Z_r^{21}}{Z_L} & 1 & \cdots & -\frac{Z_r^{2N}}{Z_L} \\ \vdots & \vdots & \ddots & \vdots \\ -\frac{Z_r^{N1}}{Z_L} & -\frac{Z_r^{N2}}{Z_L} & \cdots & 1 \end{bmatrix} \begin{bmatrix} V_1 \\ V_2 \\ \vdots \\ V_N \end{bmatrix}. \quad (14)$$

For a general antenna array, the excitation source is not applied directly to the antenna feed ports and the antennas are excited by an external plane wave source [24]. In [27] is summarized the basic criteria for the far-field region R for electromagnetic fields from radio frequency sources in the microwave range, including antennas for cell phones, microwave radar and other cases. They are

$$R > \frac{2D_x^2}{\lambda}, \quad R \gg D_x \quad \text{and} \quad R \gg \lambda, \quad (15)$$

in which D_x is the largest linear dimension of the antenna. Only when all the above inequalities are satisfied, one obtains the far-field condition [27].

IV. MICROSTRIP ANTENNA DESIGN

One of the characteristics of an antenna array is the irradiation, or the emission of electromagnetic waves in space, efficiently [28], in addition to receiving these waves. As the quality of the transmitted signal increases, the reliability of the system also increases. A system with antenna arrays can contribute to this by increasing the number of users that can be managed and adding the number of services that the system can offer [29].

Usually, the array elements are identical in their geometric form and their most common geometric configuration are linear, circular, rectangular and spherical [30]. The MC and the spatial correlation

between the elements are factors that have implication on the distance D between the elements. It is recommended that $D \geq \lambda/2$ [30].

Microstrip antennas consist of a thin metallic blade, usually 0.035 mm of thickness, built on a dielectric substrate, with a ground plane on the underside substrate. The rectangular patch is the most used antenna configuration. The radiating elements and power lines are, in general, photographed on the dielectric substrate. The patch can also be square, circular, elliptical, triangular or any shape. The most used feeding methods are the microstrip line, the coaxial probe, opening coupling and proximity coupling [30]. The rectangular patch model with a microstrip feed line is considered in this work due to its good performance, easy analysis and wide use. The design of a eight-element microstrip antenna is defined according to Fig. 3.

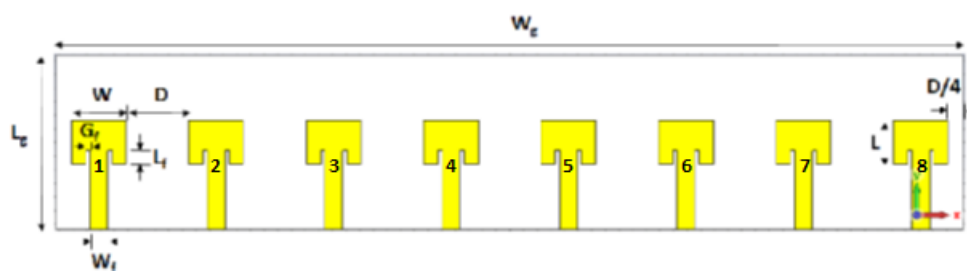


Fig. 3. Microstrip antenna in front view.

Fig. 3 shows the physical parameters for antenna design, W and L are the width and length of patch, respectively, W_g and L_g are the width and the length of the ground plane, respectively. They are defined as

$$W_g = 4 \times W + 3,5 \times D \quad \text{and} \quad L_g = 4 \times L. \quad (16)$$

The width and length of the ground plane is equal in size to the width and length of the substrate, respectively. The width of the feed line is W_f , L_f is the length of the radiant gap within the patch and G_f is the width of the gap. The distance between the elements is represented by D , and the parameters W , L , W_f , L_f and G_f are optimized in this study to minimize the antenna size.

The most suitable substrates for the good performance of the antenna must have a low dielectric constant [30], ϵ_r , in the range of 2.2 to 12 and h_s , its thickness, corresponds to a small fraction of the wavelength, usually $0.003\lambda \leq h_s \leq 0.05\lambda$. The thickest substrates have shown a better performance [30]. Based on these recommendations, the substrate chosen was the RO 3003[®] by Rogers Corporation which has a dielectric constant $\epsilon_r = 3$, dissipation factor $\tan(\delta) = 0.0010$ (for 10 GHz and 23°C) and $h_s = 0.5$ mm [31].

The frequency of 26 GHz is defined for system evaluation and the parameters of microstrip antenna are optimized according to the goals:

- 1) Resonance frequency f_o at 26 ± 0.5 GHz (the closer);
- 2) Reflection coefficient (Parameter S) < -10 dB (the smaller);
- 3) Voltage Standing Wave Ratio (VSWR) < 2 (the smaller the better);
- 4) Frequency band B > 0.6 GHz (the higher);
- 5) Internal impedance Z_{in} at 50 Ω (the closer);

6) Substrate width $W_g < 67.3$ mm, width of the smartphone iPhone 8 (the smaller).

The reflection coefficients in decibel (S parameters) are evaluated, which must be less than -10 dB for a resonance frequency the closest possible to 26 GHz. The VSWR, which must be less than two and ensure a bandwidth close to 1 GHz. And the Z parameters, that is, the self-impedance of each element and the mutual impedance between them. The self-impedance must be close to 50Ω to guarantee a good impedance match.

V. BIO-INSPIRED ALGORITHMS

John Holland [32] proposed the method that transforms a population of individuals or chromosomes into a new population that uses the Darwinian principle of reproduction and survival of the fittest, as happens naturally in the genetic operations of crossing and mutation [33]. Each individual in a population is associated with a fitness values, which represents a possibility of solving the proposed problem. A search that uses a GA seems to be adequate to find the best solution to the problem based on the genetic operators of selection, crossover and mutation.

Kennedy and Eberhart proposed the PSO algorithm [34] from the particle swarm concept to solve computational intelligence problems [35]. The speed and the particle position are attributes of the algorithm's objective function [36]. The updating of the speed and particle position show the best solution.

Fig. 4 presents a complete flowchart of the working methodology, using bio-inspired algorithms. The parameters of the microstrip antenna, with a rectangular patch, are optimized using a GA and the PSO to maximize the channel throughput and the distance among the elements.

Initially, the physical and electrical parameters are inserted in the microstrip antenna simulator and defined according to design recommendations for this type of antenna. The simulation and the results of the antenna behavior are performed and evaluated in the CST Studio Suite[®] software, it is verified if the expected values are reached and, otherwise, the optimization is carried out with variation of some physical parameters until the goal is reached.

For designing the microstrip antenna, the application area "MW & RF & Optical" for Antennas is chosen, considering patch antennas. The solution used is in time domain, which includes finite integration technique (FIT) and transmission line matrix (TLM) in the same package. E-field, H-field and Farfield monitors are set for performance analysis in 26 GHz. After that, the microstrip antenna is designed with optimization of the size of its physical characteristics.

With the data collected from this first simulation, the MIMO system simulator runs in Matlab[®] programming language and is initiated seeking to reduce the distance between the elements that promote the highest channel throughput. The optimization algorithm is executed until it finds the shortest distance or a defined stop point. The MIMO system block receives from the previous procedure the values of the parameters: frequency of operation, number of array elements, internal and load impedances of the antennas, Z parameters and distance between the elements. The SNR values are added to evaluate capacity in function of its variation. After that, an evaluation is made, using the Equations 2, 10 and 14, as to whether the smallest antenna in terms of width has already been found according to commercial smartphones standards. If not, the process is restarted for a new antenna design.

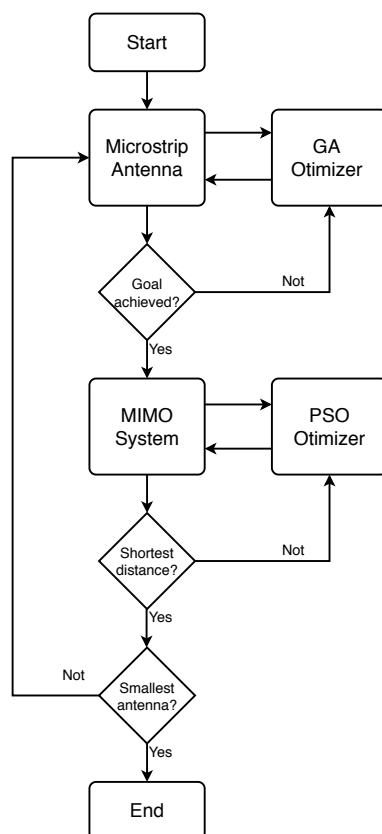


Fig. 4. Complete flowchart of the methodology.

TABLE I. GA OPTIMIZATION PARAMETERS.

Parameter	GA
Population size	20 individuals
Total generations	1000
Results	uniform distribution
Objective function level	0
Mutation rate	0.6

A. Simulations Setup

The values of the algorithms configuration parameters are shown in Tables I and II. The maximum and minimum configuration value of the PSO parameters are shown in Table II, in which c_1 is the cognitive acceleration coefficient and c_2 is the social acceleration coefficients. A uniform distribution is used to obtain the random values r_1 and r_2 . The inertia weight ω is used to control the particle's speed and to avoid its explosions during the process. The most commonly used strategy is to initialize the search process with ω close to one and reduce it linearly during all the process [37]. In this paper, the local search space was reduced to distances less than $\lambda/2$, values greater than this solution are not important because the MC effect is already considered. After this, the acceleration rate δ is experienced increasing or decreasing the acceleration coefficients, the δ value is obtained from a uniform distribution between 0.05 and 0.10. In strategies in which a slight increase or decrease in the acceleration coefficients is required, a ratio of 0.5δ is used.

TABLE II. PSO OPTIMIZATION PARAMETERS.

Parameter	PSO
Swarm size	50 particles
Operator	Mutation
Mutation rate (%)	1.0
c_{1max} and c_{1min}	2.5 and 1.5
c_{2max} and c_{2min}	2.5 and 1.5
r_{1max} and r_{1min}	1.0 and 0.0
r_{2max} and r_{2min}	1.0 and 0.0
ω_{max} and ω_{min}	0.9 and 0.4
δ_{max} and δ_{min}	0.1 and 0.05

TABLE III. RESULTS OF THE PARAMETERS FOR MICROSTRIP ANTENNA.

Parameter	Initial Value	Optimized Value	Final Value
W (mm)	4.1	3.98	4.0
L (mm)	2.9	3.23842	3.2
W_f (mm)	1.2	1.29729	1.3
L_f (mm)	1.5	1.00143	1.0
G_f (mm)	0.3	0.294	0.3
D (mm)	6.0	4.62692	4.6
W_g (mm)	77.8	66.54175	66.5
L_g (mm)	11.6	12.85368	12.8

VI. RESULTS

After the whole design optimization process for the microstrip antenna and the MIMO system, and after the evaluation and rounding, the final values of the physical parameters for the microstrip antenna are described in Table III.

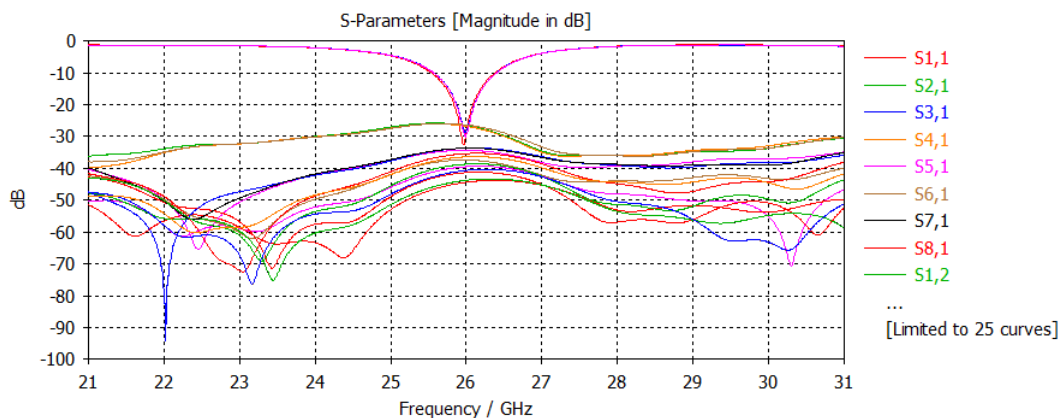
It is possible to observe a change in the values of each parameter and a reduction of 14.5% in W_g , which is one of the goals established in the limit of 67.3 mm. This happens, mainly, due to the reduction of W and D values.

Fig. 5(a) and 5(b) show the values of the S parameters between each element and in itself and, due to software limitations, only the first 25 curves are shown. Fig. 6(a) and 6(b) show the values of the S parameters in the resonance frequency.

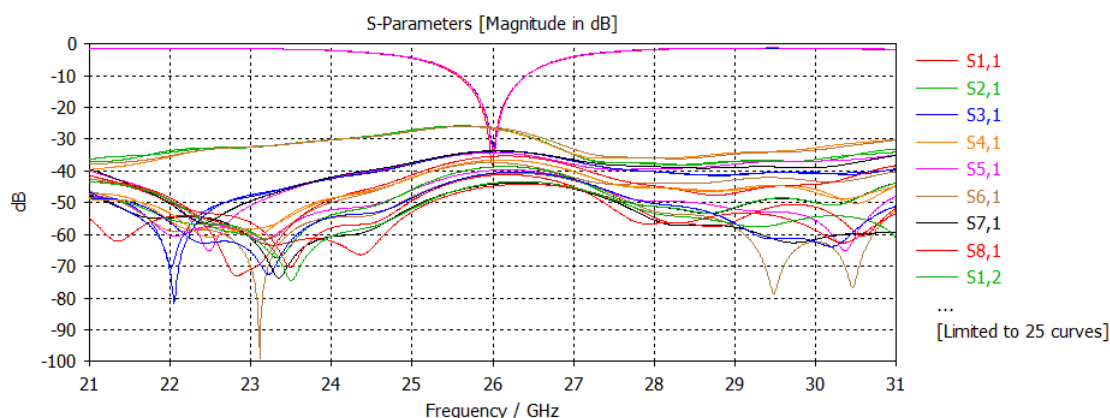
It is possible to observe from the graphs the efficiency of the GA algorithm in the search for the values of the S parameters and the resonance frequency for all elements.

Table IV shows the response of the design objectives of the microstrip antenna after optimization. It is possible to observe that the optimization method achieved five of the six design objectives with efficiency. The resonance frequency, the reflection coefficients (S parameters), the VSWR, the bandwidth and the substrate width achieved better than expected values. The line reference impedance used in this research is 50Ω . The algorithm didn't achieve optimal values of internal impedance that would promote a perfect impedance match with the transmission line, but this is a non-complex problem to solve with an adequate design of transmission line with stub and will be the subject of future works.

The far-field measurement graphs were evaluated to analyze the gain, directivity and efficiency of



(a) *S* Parameters in transmission mode.



(b) *S* Parameters in reception mode.

Fig. 5. Results of the *S* parameters *S* with all the antenna elements.

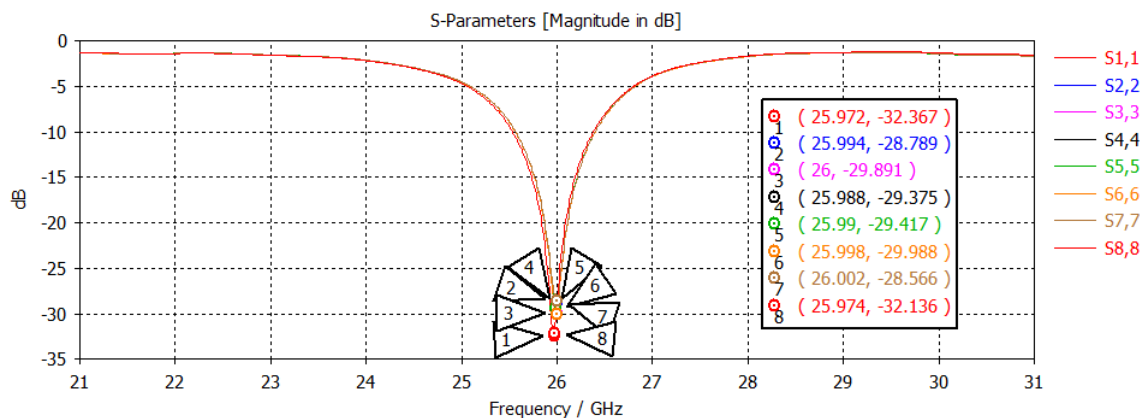
TABLE IV. RESULTS OF THE DESIGN GOALS FOR THE MICROSTRIP ANTENNA.

Parameters	Goals	Initial Value	Results	
			TX Mode	RX Mode
f_o	26 ± 0.5 GHz	27.3 GHz	26 ± 0.028 GHz	26 ± 0.017 GHz
<i>S</i>	< -10 dB	-7.1 dB	< -28.5 dB	< -32.5 dB
VSWR	< 2	9.5	1.06	1.04
B	> 0.6 GHz	0	0.9 GHz	0.9 GHz
R_{in}/Z_{in}	50 Ω	31.9 Ω	$(28.5 + j1.7)$ Ω	$(29.7 + j0.8)$ Ω
W_g	< 67.3 mm	77.8 mm	66.5 mm	66.5 mm

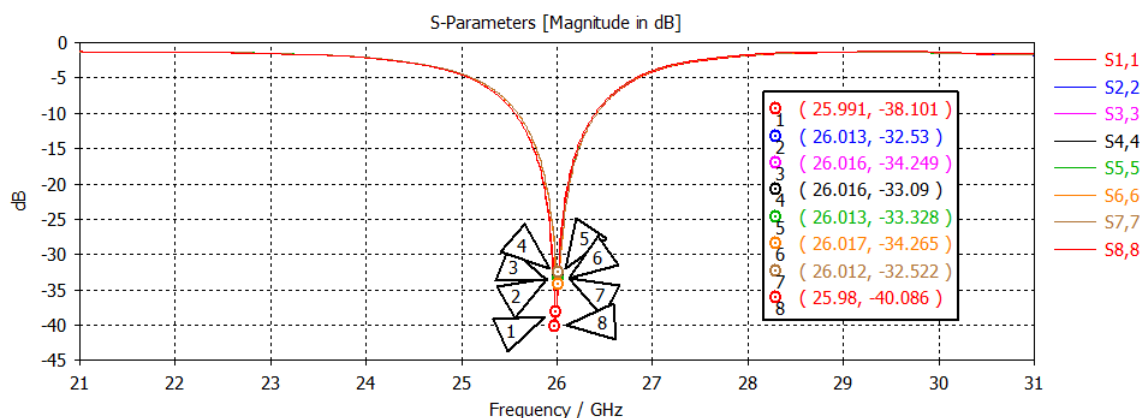
the antenna, and are presented in Fig. 7(a) and 7(b).

The antenna presents good directivity with a gain of 7.24 dBi in the frequency of 26 GHz, and also has good efficiency. In this paper, the distance between the elements of the transmitting antenna array was fixed at a wavelength (λ) and this distance in the receiving antenna elements was varied from 0.001λ to 1λ . Table V details the values of throughput optimization versus distance reduction for a MIMO 8×8 system with a signal-noise-ratio (SNR) of 20 dB.

The displacement behavior of the elements can be observed, with and without optimization, showing that the method is valid to achieve higher channel throughputs for a distance smaller than $\lambda/2$. There



(a) *S* Parameters at the resonance frequency in transmission mode.



(b) *S* Parameters at the resonance frequency in reception mode.

Fig. 6. Results of the *S* parameters *S* with all the antenna elements.

TABLE V. RESULT OF THE CHANNEL THROUGHPUT OPTIMIZATION IN MIMO 8×8 SYSTEM AS A FUNCTION OF DISTANCE.

Method	Throughput (bits/s/Hz)	Shortest Distance (λ)	Increase (%)
Without optimization	40.38	0.522	-
With optimization	44.89	0.401	11.1

was a reduction in the distance between the elements by 23.7%, which represents, at a frequency of 26 GHz, a reduction of 10.5 mm in the total width of the microstrip. Also, at a distance between the elements of 0.401λ , there is an increase of 11.1% in channel throughput.

The response of the throughput optimization of the MIMO systems implemented as a function of the SNR can be seen in Fig. 8.

To calculate the throughput, the smallest distance between the elements found by the algorithm is considered, in this case, 0.401λ , for the transmitter and receiver mode, simulating two mobile stations with the microstrip antennas designed. It is possible to observe that the increase in SNR also increases the capacity optimization, that is, the higher the SNR, the better the application of this method. And

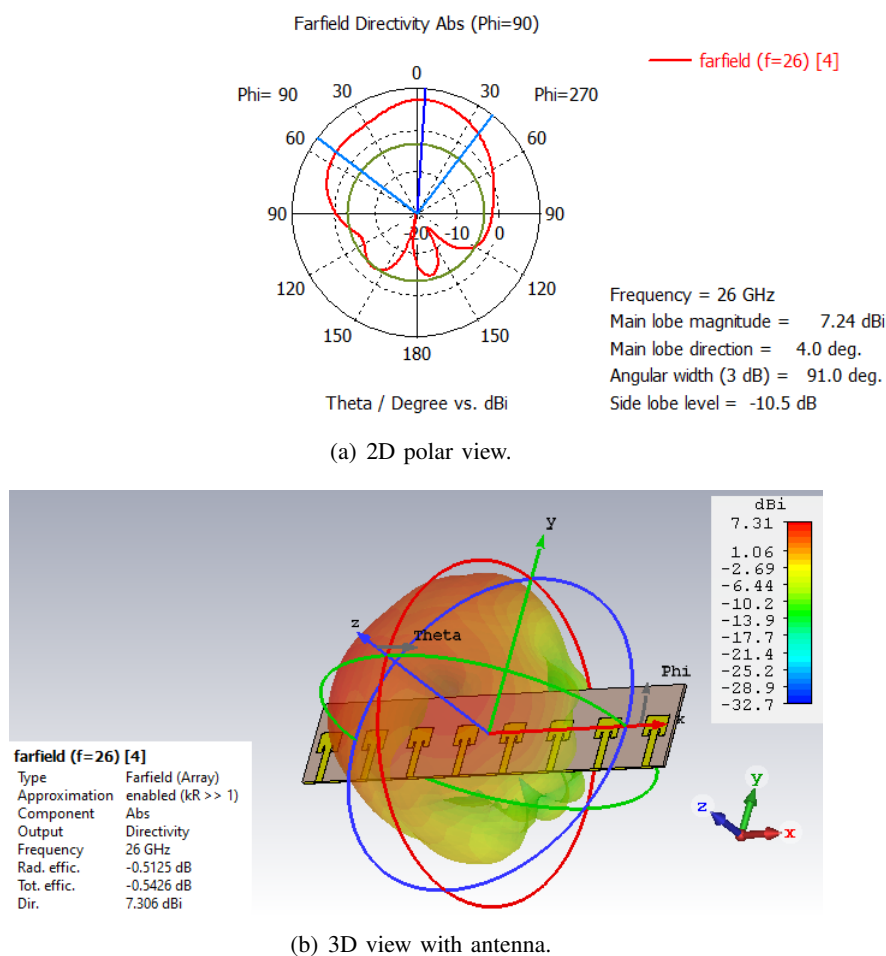


Fig. 7. Far-field radiation diagram for microstrip antenna.

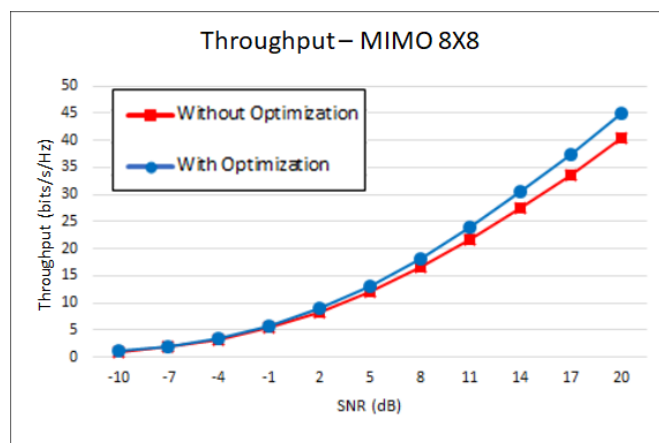


Fig. 8. Comparison graph of throughput as a function of SNR in receiver mode with and without optimization.

once again the increase in channel capacity of 11.1% for a 20 dB SNR is confirmed.

The results confirm the efficiency of the algorithm in solving the throughput optimization problem with reduction of the distance between the elements considering the MC. They also show that a well founded methodology combined with artificial intelligence methods can generate satisfactory results and reduce computational complexity.

VII. CONCLUSION

This paper presents a methodology to increase the channel throughput of a MIMO system, considering the mutual coupling effect, with the use of bio-inspired algorithms in the optimization process. Another objective of this study was to minimize the size of the microstrip antenna, based on considerations about the distance between the elements and on the physical dimensions of the antenna. The rectangular patch with transmission line was chosen as a template. The physical parameters of the antenna and some performance measures were evaluated, such as: operating frequency, parameters S and Z , VSWR, internal resistance, directivity, gain and efficiency.

The GA and PSO algorithms form a simple and powerful tool to minimize the size of the antenna and optimize the channel throughput for MIMO systems. The best results show an increase of 11.1% in the throughput of MIMO channels 8×8 with the PSO algorithm, including a proposal to modify the search strategy of the algorithm and a reduction in the distance between the antenna elements by 23.7%.

For future works, the authors plan to extend the methodology to other frequency bands, including millimeter waves, such as 28 and 30 GHz. The study of mutual coupling in the reception mode must be further compared with other methods from the literature, as well as, the effect of this methodology for non-uniform distances between the antenna elements. Impedance matching solutions will also be studied, for the proposed antenna.

ACKNOWLEDGMENTS

The authors would like to thank the Institute for Advanced Studies in Communications (Iecom), the Brazilian Council for Research and Development (CNPq), the Coordination for the Improvement of Higher Education Personnel (CAPES), and the Postgraduate Office (Copele) of the Federal University of Campina Grande (UFCG) for providing support for this work.

REFERENCES

- [1] GSMA, "The mobile economy," February 2022, <https://www.gsma.com/mobileeconomy/wp-content/uploads/2022/02/280222-The-Mobile-Economy-2022.pdf>, Acessado em 05/dez/2022.
- [2] I. A. C. Leal, M. Alencar, and W. Lopes, "Genetic algorithm optimization applied to the project of MIMO systems," in *25th International Conference on Software, Telecommunications and Computer Networks – SoftCOM*, pp. 1–5, September 2017.
- [3] H. Wei, D. Wang, H. Zhu, J. Wang, S. Sun, and X. You, "Mutual coupling calibration for multiuser massive MIMO systems," *IEEE Transactions on Wireless Communications*, vol. 15, no. 1, pp. 606–619, January 2016.
- [4] J.-H. Lee and J.-Y. Lee, "Optimal beamforming-selection spatial precoding using population-based stochastic optimization for massive wireless MIMO communication systems," *Elsevier*, vol. 354, pp. 4248–4271, 2017.
- [5] M.-H. Ho, C.-C. Chiu, and S.-H. Liao, "Optimisation of channel capacity for multiple-input multiple-output smart antenna using a particle swarm optimiser," *IET Communications*, vol. 6, no. 16, pp. 2645–2653, 2012.
- [6] J. Jayasinghe, J. Anguera, and D. Uduwawala, "Genetic algorithm optimization of a high-directivity microstrip patch antenna having a rectangular profile," *Radioengineering*, vol. 22, no. 3, 2013.
- [7] M. Lamsalli, A. El Hamichi, M. Boussois, N. Amar Touhami, and T. Elhamadi, "Genetic algorithm optimization for microstrip patch antenna miniaturization," *Progress In Electromagnetics Research*, vol. 60, pp. 113–120, 2016.
- [8] R. G. Mishra, R. Mishra, P. Kuchhal, and N. P. Kumari, "Optimization and analysis of high gain wideband microstrip patch antenna using genetic algorithm," *International Journal of Engineering & Technology*, vol. 7, no. 1.5, pp. 176–179, 2018.
- [9] P. Kumar and M. S. Patterh, "Linear antenna array optimization using genetic algorithm," *International Journal For Technological Research In Engineering*, vol. 2, no. 11, pp. 2347–4718, July 2015.

- [10] A. E. Forooshani, A. A. Lotfi-Neyestanak, and D. G. Michelson, "Optimization of antenna placement in distributed MIMO systems for underground mines," *IEEE Transactions on Wireless Communications*, vol. 13, no. 9, pp. 4685–4692, September 2014.
- [11] I. A. C. Leal, W. T. A. Lopes, and M. S. Alencar, "Projeto de sistemas MIMO utilizando otimização por enxame de partículas," in *XXXV Simpósio Brasileiro de Telecomunicações – SBrT*, Setembro 2017.
- [12] M. Cui, W. Zou, Y. Wang, and R. Zhang, "Hybrid precoding for millimetre wave MIMO systems based on particle swarm optimisation," *IET Communications*, vol. 13, no. 11, pp. 1643–1650, May 2019.
- [13] J. Sharony, "Introduction to wireless MIMO – theory and applications," Center of Excellence in Wireless and Information Technology, Stony Brook University, Tech. Rep., November 2006.
- [14] E. Biglieri, R. Calderbank, A. Constantinides, A. Goldsmith, A. Paulraj, and H. V. Poor, *MIMO Wireless Communication*, 1st ed. Cambridge, UK: Cambridge University Press, 2007.
- [15] X. Liu and M. E. Bialkowski, "Effect of antenna mutual coupling on MIMO channel estimation and capacity," *International Journal of Antennas and Propagation*, vol. 2010, pp. 1–9, 2010, article ID 306173.
- [16] A. Goldsmith, *Wireless Communication*, 1st ed. New York, USA: Cambridge University Press, 2005.
- [17] T. Brown, E. Carvalho, and P. Kyritsi, *Practical Guide to the MIMO Radio Channel with Matlab® Examples*, 1st ed. Noida, India: Wiley, 2012.
- [18] N. Almeida, S. Mota, and A. Rocha, "Modelação do canal rádio MIMO," *Eletrônica e Telecomunicações*, vol. 5, no. 2, pp. 129–135, June 2010.
- [19] B. Han and Y. R. Zheng, "Higher rank principal Kronecker model for triply selective fading channels with experimental validation," *IEEE Transactions on Vehicular Technology*, vol. 64, no. 5, pp. 1654–1663, May 2015.
- [20] W. J. L. Queiroz, F. Madeiro, W. T. A. Lopes, and M. S. Alencar, "Spatial correlation for DoA characterization using Von Mises, Cosine and Gaussian distributions," *International Journal of Antennas and Propagation*, vol. 2011, pp. 1–12, 2011.
- [21] I. A. C. Leal, M. S. Alencar, and W. T. A. Lopes, "Particle swarm optimization applied to control of mutual coupling in MIMO systems," in *IEEE Latin-American Conference on Communications – LATINCOM*, 11 2019.
- [22] S. Lu, H. T. Hui, and M. Bialkowski, "Optimizing MIMO channel capacities under the influence of antenna mutual coupling," *IEEE Antennas and Wireless Propagation Letters*, vol. 7, no. 1, pp. 287–290, 2008.
- [23] I. J. Gupta and A. A. Ksienski, "Effect of mutual impedance for application in dipole receiving antenna arrays," *IEEE Transactions on Antennas and Propagation*, vol. 5, no. AP-31, pp. 785–791, 1983.
- [24] H.-S. Lui, H. T. Hui, and M. S. Leong, "A note on the mutual-coupling problems in transmitting and receiving antenna arrays," *IEEE Antennas and Propagation Magazine*, vol. 51, no. 5, pp. 171–176, 2009.
- [25] H. T. Hui, "A new definition of mutual impedance for application in dipole receiving antenna arrays," *IEEE Antennas and Wireless Propagation Letters*, vol. 3, no. 1, pp. 364–367, 2004.
- [26] Y. Yu, H.-S. Lui, C. H. Niow, and H. T. Hui, "Improved DoA estimations using the receiving mutual impedances for mutual coupling compensation: An experimental study," *IEEE Transactions on Wireless Communications*, vol. 10, no. 7, pp. 2228–2233, 2011.
- [27] W. L. Stutzman and G. A. Thiele, *Antenna theory and design*. John Wiley & Sons, 2012.
- [28] M. N. O. Sadiku, *Elementos de Eletromagnetismo*, 3rd ed. Porto Alegre: Bookman, 2004.
- [29] M. S. Alencar and W. J. L. Queiroz, *Ondas Eletromagnéticas e Teoria de Antenas*, 1st ed. São Paulo: Érica, 2010.
- [30] C. A. Balanis, *Antenna Theory, Analysis and Design*, 4th ed. New Jersey, USA: Wiley, 2016.
- [31] Rogers, "Data sheet: Ro3000 series circuit materials," 92-130, Rogers Corporation, USA, Tech. Rep., 2019.
- [32] J. H. Holland, *Adaptation in Natural and Artificial Systems*, 3rd ed. Cambridge, MA, USA: MIT Press, 1993.
- [33] J. R. Koza, "Survey of genetic algorithms and genetic programming," in *Wescon Business Conference*, pp. 589–595, November 1995.
- [34] J. Kennedy and R. Eberhart, "Particle swarm optimization," in *Proceedings of IEEE International Conference on Neural Networks*, 1995.
- [35] I. A. C. Leal, D. R. C. Silva, D. A. R. Chaves, and C. J. A. Bastos-Filho, "Bio-inspired optimization of blocked calls in cellular mobile systems," in *International Workshop on Telecommunications (IWT'2015)*, pp. 1–6, June 2015.
- [36] D. Le and G. Nguyen, "A novel particle swarm optimization-based algorithm for the optimal centralized wireless access network," *International Journal of Computer Science Issues*, vol. 10, no. 1, pp. 721–727, 2013.
- [37] R. Eberhart and Y. Shi, "Comparing inertial weights and constriction factors in particle swarm optimization," in *Congress Evolutionary Computation*, pp. 84–88, July 2000.